To Appear :Philosophical Transactions of the Royal Society (A).
Accepted for publication September 25 (2017)
DOI 10.1098/rsta.2017.0151.

Statistical Mechanics of Binary Mixture Adsorption in Metal-Organic Frameworks in the Osmotic Ensemble.

Lawrence J. Dunne [a,c,d*], George Manos[b]

[a] School of Engineering, London South Bank University, London SE1 0AA, UK.

[b] Department of Chemical Engineering, University College London, Torrington Place, London, WC1E 7JE, UK.

[c] Department of Materials, Imperial College London, London SW7 2AZ, UK

[d]Department of Chemistry, University of Sussex, Falmer, Brighton, BN1 9QJ, UK

KEYWORDS: metal–organic framework, mixture adsorption isotherms, transfer-matrix, osmotic ensemble, binary and co-adsorption, mechanical pressure.

Abstract

Although crucial for designing separation processes little is known experimentally about multi-component adsorption isotherms in comparison with pure single components. Very few binary mixture adsorption isotherms are to be found in the literature and information about isotherms over a wide range of gas phase composition and mechanical pressures and temperature is lacking. Here we present a quasi-one dimensional statistical mechanical model of binary mixture adsorption in metal-organic frameworks (MOFs) treated exactly by a transfer matrix method in the Osmotic Ensemble. The experimental parameter space may be very complex and investigations into multi-component mixture adsorption may be guided by theoretical insights. The approach successfully models breathing structural transitions induced by adsorption giving a good account of the shape of adsorption isotherms of CO_2 and CH_4 adsorption in MIL-53(Al). Binary mixture isotherms and co-adsorption phase diagrams are also calculated and found to give a good description of the experimental trends in these properties and because of the wide model parameter range which reproduces this behaviour suggests that this is generic to MOFs. Finally a study is made of the influence of mechanical pressure on the shape of CO_2 and CH_4 adsorption isotherms in MIL-53(Al). Quite modest mechanical pressures can induce significant changes to isotherm shapes in MOFs with implications for binary mixture separation processes.

*Corresponding Author: dunnel@lsbu.ac.uk

1. Introduction

Solvable statistical mechanical models such as the Ising model, even when somewhat physically unrealistic, have played a very significant role in the theory of condensed phases. Here we discuss a development in the statistical mechanics of binary mixture adsorption. In this special memorial issue 'Modern Theoretical Chemistry' which celebrates John Murrell's contribution to theoretical physics and chemistry it is appropriate to discuss binary mixture adsorption as he had a deep interest in statistical mechanics. We were privileged to have worked with him over many years on topics ranging from the theory of superconductivity to models of melting and the statistical mechanics of fluids[1,2,3].

Finding viable separation procedures for binary component mixtures is a challenging and important problem and a consideration in the development of 'green technologies' where for example carbon dioxide needs to be separated from methane in natural gas[4,5,6,7,8]. Carbon dioxide separation is also a central issue in carbon sequestration for the mitigation of climate change[9]. Although crucial for designing separation processes relatively little is known experimentally about multi-component adsorption isotherms. Very few binary mixture adsorption isotherms are to be found in the literature over a wide range of composition, pressure and temperature. The parameter space can be challengingly complex and experimental design may be guided by theoretical insights. Multicomponent adsorption isotherms may exhibit counter-intuitive features which when accompanied by possible structural transitions make a rich variety of behaviours possible[10].

Recently significant attention has been focused on metal-organic frameworks (MOFs) which are an important group of hybrid organic-inorganic nanoporous solids with remarkable adsorption and structural properties. MOFs constitute a family of soft porous crystals, described by Kitagawa and co-workers[11] as "porous crystals that possess both a highly ordered network and structural transformability". Metal-Organic Frameworks (MOFs) have high potential for use in adsorptive separation processes[12,13,14,15,16,17,18,19,20,21] due to the unique characteristics of structural pores which may be adapted to permit adsorption to take place on the basis of molecular shape and size and in particular structural flexibility[22,23,24,25,26,27,28]. In MOFs metal framework centres and organic units link thereby allowing structural transitions to occur upon gas adsorption[29,30,31,32,33,34]. Temperature and pressure can also induce structural transitions[32,33,35]. Coudert and co-workers[36] classify guest induced structural transitions into gate opening and breathing, which they define as two successive transitions, from a large pore (LP) to a narrow pore (NP) state and back again to the LP state. Despite great interest in mixture adsorption in MOFs, adsorption data is still extremely scarce because of the challenge of undertaking comprehensive measurements. Baron and co-workers[37] have reported measurements of isotherms of methane/carbon dioxide adsorption in MIL(53)Al which we have modelled here. However, we do not consider specific MOF structural details but

focus on developing a statistical mechanical model which mimics the essential features of mixture adsorption in these materials. Mixture adsorption in MOFs has been extensively studied by Coudert and co-workers[38,39]. They have made significant advances in the development of the theory of mixture adsorption in MOFs[38]. They presented an experimental and theoretical study of CO_2/CH_4 mixture co-adsorption and breathing in the metal-organic framework MIL-53(Al)[39]. Successful co-adsorption predictions were made from pure-component adsorption data using the Osmotic Framework Adsorption Solution Theory (OFAST). The co-adsorption phase diagrams derived show surprising characteristic features which we will discuss below as these are reproduced by our model.

Llewelyn and co-workers[28] and Gomez et al[40] have also reported measurement of 1:1 methane/carbon dioxide adsorption in MIL(53)Cr and MIL(53)Al respectively which will concern us here. Other relevant simulations are those of Snurr and co-workers[41].

Thus, in this article we discuss the development of an exactly soluble lattice model of binary gas mixture adsorption in MOFs in the osmotic ensemble. The osmotic ensemble was developed initially by Brennan and Madden[42] and Panagiotopoulos[43]**.** The theoretical approach taken here is a natural development of our earlier presentation of an exactly solvable statistical mechanical lattice model of a MOF in the Osmotic ensemble using a transfer matrix method which treats the solid and gas component on an equal footing[44]. We previously only considered a single component but here we consider mixture adsorption in MOFs and develop a phenomenological lattice model which is parameterized against single component adsorption isotherms. These parameters are then used to predict mixture adsorption characteristics and comparisons made with the Coudert results and the experimental studies of Barron et al[37] for MIL-53-(Al) for CO_2/CH_4 mixture adsorption and Gomez et al.[40]

Our approach cannot compete with more computationally demanding methods such as Monte-Carlo simulations which treat three dimensional crystals. We do not expect the semi-empirical parameters found for our quasi-one dimensional model to accurately describe binary mixture adsorption in a real MOF. In comparison to more computationally based approaches which model three dimensional crystals our methodology has a different purpose and value. Our exactly treated statistical mechanical models may readily afford original predictions of novel behaviour of these widely studied systems. Hence, our objective is to devise a model which enables the broad features of binary mixture adsorption isotherms to be studied quickly and cheaply. Furthermore, exactly treated statistical mechanical models may provide novel insights into these phenomena. We also investigate the influence of mechanical compression on mixture isotherm which as far as can be checked is new.

2. Quasi-one Dimensional Model of Binary Mixture Adsorption in Metal-Organic Frameworks.

Recently we have developed an exactly solvable transfer matrix treatment of statistical mechanical lattice model of a MOF which enables single component adsorption isotherms and the compression of these flexible soft materials to be modelled[45]. Here we extend this accurate transfer matrix treatment of a quasi-one dimensional statistical mechanical Osmotic ensemble model of pressure and adsorption induced structural transitions in MOFs to mixtures. We give a full analysis of the extension of the theory to mixture adsorption. The calculation of the Osmotic Potential requires the solution of a matrix eigenvalue problem which may be treated numerically or exactly in some instances. It is found that for weak unit-cell interactions it is possible to obtain all the eigenvalues of the osmotic ensemble transfer matrix for a binary mixture adsorbed in a MOF by an analytical approach. The theory then allows a wide range of chemical and physical features to be modelled.

It is widely felt that the most valuable ensemble to study adsorption in soft expandable materials is the osmotic ensemble[42,43]**.** Coudert and co-workers[46,38,47] developed the osmotic ensemble for molecular simulation studies of adsorption in MOF. In his classic book Hill[48] formulated a number of 'Generalized Ensembles' and the Osmotic ensemble falls into this classification. For this ensemble the independent thermodynamic variables for a binary mixture adsorption are the temperature, T, the number of gas adsorbing unit cells N in the MOF, the mechanical pressure σ and the chemical potentials μ_a, μ_b of the adsorbed gas species *a,b.* The set of chemical potentials μ_a, μ_b and mechanical pressure σ can be considered as independent thermodynamic control variables.

We focus on a chain of N groups of unit cells each with a finite volume discussed below, which may be in either a large pore (LP) or narrow pore (NP) conformation. The chain extends in the x-direction and is subjected to a mechanical compressive stress σ (loosely termed pressure) directed along this axis as shown in Figure. 1. If no external mechanical stress is applied σ is equal to the gas pressure P but otherwise σ and P can be independently varied. The mechanical stress or pressure term σ includes that exerted by the gas pressure P along the ends of the chain. This is evidently an unrealistic description of a three dimensional crystal in contact with a gas reservoir but nevertheless gives a tractable model providing useful insights into adsorption in MOFs.

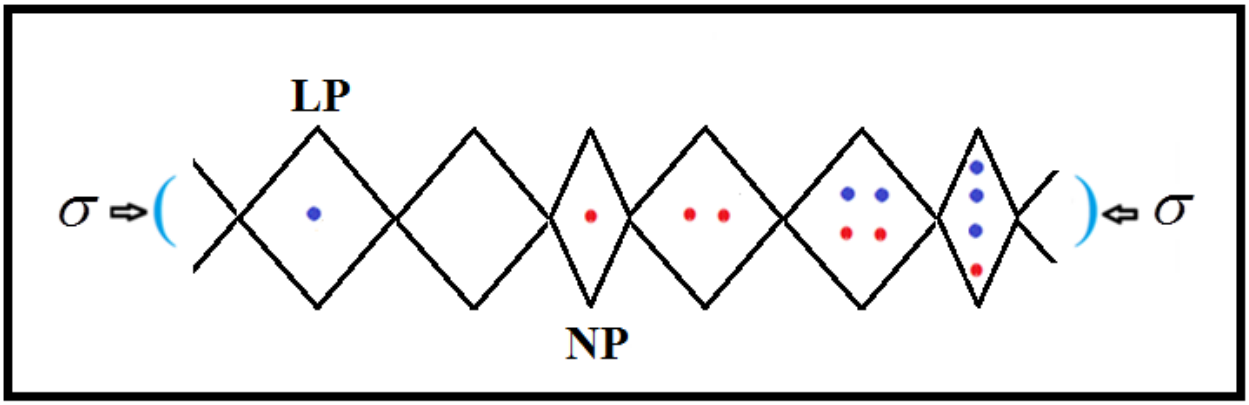

Fig. 1 An example of a typical configuration of a group of species considered in the infinite quasi-one dimensional chain. All possible occupations and configurations are allowed in the model. The structure is subjected to a mechanical compressive stress σ (pressure) directed along the x -axis. The large pore (LP) on the far left contains 1 methane molecule (blue); the next LP to the right is vacant, while the neighbour narrow pore (NP) on the right contains 1 carbon dioxide molecule (red). The NP on the far right contains 3 methane molecules (blue) and 1 carbon dioxide molecule and so on. Both types of molecules are treated as spheres. All energetically possible configurations and cell occupations are considered.

The adsorbed molecules occupying the cells are in equilibrium with those in a gas reservoir at pressure *P* and temperature *T*. The gas phase mole fractions of components *a*,*b* are denoted by X and (1-X) respectively. The chemical potential μ_a of component *a* is expressed for convenience as $\mu_a = \mu^0{}_a + kT\ln(XP)$ where the standard chemical potential $\mu^0{}_a$ is given[48] by $\mu^0{}_a = -kT\ln\left[\left(\frac{2\pi m_a kT}{h^2}\right)^{3/2} kT\right]$ and where modification for non-ideal behaviour is straightforwardly achieved by replacing pressure by fugacity. (Note that the arguments of the two logarithmic terms defining μ_a have the dimensions of pressure, allowing the chemical potential to be expressed if desired as a single term with dimensions of energy. This point is discussed by Hill[49]). m_a is the molecular mass, *k* is Boltzmann's constant and *h* is Planck's constant. Similar expressions exist for component *b*.

Each unit cell may be occupied by a mixture of methane/carbon dioxide molecules so that all possible occupations and configurations are allowed in the model.

For the mixture of species adsorbed in the one-dimensional chain of *N* unit cells, the Osmotic Partition function $\Phi(\sigma, T, \mu_a, \mu_b)$ may be expressed as:

$$\Phi(\sigma, T, \mu_a, \mu_b) = \sum_{V} \sum_{n_a, n_b} \exp(-\frac{\sigma V}{kT}) Q(n_a, n_b, V, T) \exp(\frac{\mu_a n_a + \mu_b n_b}{kT}) \qquad (1)$$

The summation runs over the varying volume *V* occupied by the 2 types of *N* unit cells shown in Fig. 1 and the numbers n_a, n_b of gas molecules *a*, *b*. $Q(n_a, n_b, V, T)$ is the Canonical partition function for volume *V*. The Osmotic Potential Ω used by Coudert is given by $\Omega = -kT \ln \Phi$ obtained here from the logarithm of the maximum term in the generalised partition function. In our method we calculate this exactly by a transfer matrix method thereby obtaining thermodynamic functions by using the method of the maximum term.

The method of the maximum term in which the logarithm of the sum in equation (1) is replaced by the logarithm of the maximum term can be used to evaluate the osmotic potential without making any error for all practical purposes to thermodynamic quantities. Thus, the logarithm of the maximum term may be written as

$$\ln \Phi = -\frac{\sigma V^*}{kT} + \ln Q(n_a^*, n_b^*, V^*, T) + \frac{\mu_a n_a^* + \mu_b n_b^*}{kT} \qquad (2)$$

where * signifies optimum values.

The optimum values n_a^*, n_b^*, V^* must simultaneously satisfy the extremum conditions

$$\begin{aligned} (\frac{\partial \ln \Phi}{\partial V}) &= \frac{-\sigma}{kT} + (\frac{\partial \ln Q}{\partial V}) = 0 \\ (\frac{\partial \ln \Phi}{\partial n_a}) &= (\frac{\partial \ln Q}{\partial n_a}) + \frac{\mu_a}{kT} = 0 \\ \frac{\partial \ln \Phi}{\partial n_b}) &= (\frac{\partial \ln Q}{\partial n_b}) + \frac{\mu_b}{kT} = 0 \end{aligned} \qquad (3)$$

The Reader will recognize these equations as those for pressure and the adsorbed species chemical potentials in a canonical ensemble. This demonstrates that by using the method of the Maximum term the Osmotic ensemble has degenerated as expected into a Canonical ensemble as discussed for Generalized Ensembles by Hill[48]. Differentiation of equation (2) gives

$$-d(kT \ln \Phi) = V^* d\sigma - SdT - (n_a * d\mu_a + n_b * d\mu_b) \qquad (4)$$

which yields the following relations for the optimum values:

$$V^* = -kT(\frac{\partial \ln \Phi}{\partial \sigma}) \quad , \quad n_a{}^* = kT(\frac{\partial \ln \Phi}{\partial \mu_a}) \quad , \quad n_b{}^* = kT(\frac{\partial \ln \Phi}{\partial \mu_b}) \qquad (5).$$

$\ln \Phi$ will be evaluated by a transfer matrix method which we describe in the next section.

3. Transfer Matrix Treatment of Binary Mixture Adsorption in Metal-Organic Frameworks.

We have previously reviewed matrix methods for the statistical mechanical treatment of one-dimensional lattice fluids[50]. A recent study applying matrix methods to MOFs has been presented by Simon et al[51].

The Osmotic partition function equation (1) can be written as the sum of the products of *N* factors (unit cells) given by[45]

$$\Phi = \sum_{\alpha=1}^{j} \sum_{\beta=1}^{j} \sum_{\gamma=1}^{j} ..... \sum_{\omega=1}^{j} A_{\alpha\beta} A_{\beta\gamma} A_{\gamma\delta} ..... A_{\omega\alpha} \qquad (6)$$

where the *N* summations run over the *j* clusters formed by all possible energetically allowed occupations of unit cells by adsorbed molecules. Cyclic boundary conditions have been assumed where the chain is folded on to a ring. As is usual in the matrix method we define the terms $A_{\alpha\beta}$ in (6) as the product of internal partition functions f_α for cluster α and f_β for cluster β and an interspecies exponential interaction term:

$$A_{\alpha\beta} = (f_\alpha f_\beta)^{1/2} e^{-\varepsilon_{\alpha\beta}/kT} \qquad (7)$$

where the subscripts α,β run over the species 1 to *j* and the parameter $\varepsilon_{\alpha\beta}$ is the interaction energy of nearest neighbour pairs of clusters α,β.

We have observed that the essential features of the MOF adsorption iostherms can be reproduced by introducing two limiting cases by setting selected values of $\varepsilon_{\alpha\beta}$ to either zero or infinitely repulsive as described for models A and B below.

Using the inner product rule $D_{ij} = \sum_k B_{ik} C_{kj}$ for matrix multiplication of a pair of conformable matrices **B** and **C** the Osmotic Partition function given in equation (6) can be expressed as:

$$\Phi(\sigma, T, \mu_a, \mu_b) = \sum_{\alpha=1}^{j} (\mathbf{A}^N)_{\alpha\alpha} = \mathrm{Tr}\,(\mathbf{A}^N) = \sum_{i=1}^{j} (\lambda_i)^N \qquad (8)$$

where λ_1 , λ_2 , λ_3 ,.... λ_j are the eigenvalues of the transfer matrix **A** which is given below as

$$\mathbf{A} = \begin{pmatrix} f_1 e^{-\varepsilon_{11}/kT} & \cdots & (f_1 f_j)^{1/2} e^{-\varepsilon_{1j}/kT} \\ \vdots & \ddots & \vdots \\ (f_j f_1)^{1/2} e^{-\varepsilon_{1j}/kT} & \cdots & f_j e^{-\varepsilon_{jj}/kT} \end{pmatrix} \quad (9)$$

As is usual in matrix evaluations of partition functions only the largest eigenvalue of **A** concerns us here since for large *N* equation (9) reduces to

$$\Phi(\sigma, T, \mu_a, \mu_b) = (\lambda_{\max})^N \quad (10)$$

where λ_{max} is the largest eigenvalue of the matrix **A** found as discussed below in particular circumstances.

Co-adsorption into the MOF structure can occur by several mechanisms. The large and narrow pores may be occupied simultaneously by pure CH_4 or CO_2 molecules or a mixture of these as shown in figure 1. Each type of pore has temperature dependent maximum occupation numbers $N_{\max Lpa}$, $N_{\max Lpb,}$ $N_{\max Npa,}$ $N_{\max Npb}$ for species *a,b* given in Table 1 below taken from Boutin et al[52] and are rounded to the nearest integer.

Component *a*, CO_2	$u_{LP,a}$	$u_{NP,a}$	$N_{\max Lpa}$	$N_{\max Npb}$
	(1254.0 -15.75T)k	*(-244.73 -15.789T)k*	Round*(16.8-0.025T)*	Round*(2.3-0.0002T)*
Component *b*, CH_4	$u_{LP,b}$	$u_{NP,b}$	$N_{\max Lpb}$	$N_{\max Npb}$
	(-2253.0-4.29T)k	*(-9750+20.511T)k*	Round*(19.5-0.045T)*	Round*(4.87-0.0035T)*

Table 1. The adsorption energies of the pure components and maximum occupations for the large and narrow pores are parameterized as shown below. These are valid in the approximate temperature range 200-300 K. The adsorption energies have the form *u=(f-gT)k* where *f* has dimension K and *g* is dimensionless. The maximum occupations have the form N_{max}=Round(*s-rT)* where *r* has the dimension K^{-1}.

Δ which is treated as an adjustable parameter is the energy difference required to convert from the more stable LP to the NP which is discussed further below. v_{NP} and v_{LP} are the NP and LP volumes whose values are 1000 and 1400 Å^3 giving a 40% volume difference between these 2 forms.

A model for the clusters of adsorbed molecules in the LP and NP is required for pure *a/b* molecules and mixtures of these. For pure *a* molecules absorbed in the LP we assume the existence of a cluster of molecules and vacancies occupying $N_{\max LPa}$ sites in total. With n_a molecules there are $(N_{\max LPa} - n_a)$ holes or vacancies giving rise to a configurational degeneracy from all the permutations of these species (given as the first factor on the right hand side in equation 11 below). Similar considerations apply to *b* molecules and the NP.

For the mixture in the LP we let $N_{\max LP}$ be number of accessible sites in the large pore accessible to both *a* and *b* type molecules given by and assume random mixing considering all configurations with up to $N_{\max LP}$ molecules in total. However, the maximum number of each species is restricted to not exceed the individual saturation uptakes. There are $(N_{\max LP} - n_a - n_b)$ vacancies giving rise to a configurational degeneracy (given as the first factor on the right hand side in equation 13 below) from all the permutations of all these 3 species. Again, similar considerations apply to the *b* molecules and the NP. The experimental studies of Barron et al[37] suggests that $N_{\max LP} = 10$ and $N_{\max NP} = 4$ which were used in the mixture adsorption calculations shown below.

We have estimated the number of pair interactions as $(n^2 - n)/2$ for n like molecules and *nm* for *n,m* unlike molecules. Treating carbon dioxide and methane in a spherical molecule approximation, the interaction energies J_{aa} and J_{bb} are – 245*k* and - 161*k* respectively taken from literature values and where the pre-factors are in absolute degrees (K)[53]. $J_{a,b}$ is the mean effective interaction energy between a pairs of adsorbed gas molecules *a,b* in the cluster which we treat as an adjustable parameter below .

Thus the cluster partition function f_{LP,n_a} for a LP containing n_a type *a* molecules is

$$f_{LP,n_a} = \frac{N_{\max LPa}!}{(N_{\max LP,a} - n_a)!n_a!} \exp\left(\frac{-\sigma \upsilon_{LP}}{kT}\right)\left(\exp\left(\frac{-u_{LP,a} + \mu_a}{kT}\right)\right)^{n_a} \exp\left(\frac{-J_{aa}(n_a^2 - n_a)/2}{kT}\right) \quad (11)$$

where $u_{LP,a}$ is the adsorption energy of component a in the large pore as given in Table 1 above.

Similarly, a NP cluster containing n_a type *a* molecules has a cluster partition function

$$f_{NP,n_a} = \frac{N_{\max NPa}!}{(N_{\max NPa}-n_a)!n_a!}\exp(\frac{-\sigma\upsilon_{NP}-\Delta}{kT})(\exp(\frac{-u_{NP,a}+\mu_a}{kT}))^{n_a}\exp(\frac{-J_{aa}(n_a{}^2-n_a)/2}{kT}) \tag{12}$$

with similar expressions for type *b* molecules**.**

For a LP containing n_a type *a* molecules and n_b type *b* molecules the cluster partition function is

$$f_{LP,n_a,n_b} = \frac{N_{\max LP}!}{(N_{\max LP}-n_a-n_b)!n_a!n_b!}\exp(\frac{-\sigma\upsilon_{LP}}{kT})(\exp(\frac{-u_{LP,a}+\mu_a}{kT}))^{n_a}\exp(\frac{-J_{aa}(n_a{}^2-n_a)/2}{kT}) \times (\exp(\frac{-u_{LP,b}+\mu_b}{kT}))^{n_b}\exp(\frac{-J_{bb}(n_b{}^2-n_b)/2}{kT})\exp(\frac{-J_{ab}n_an_b}{kT}) \tag{13}$$

and with similar modified expressions for the NP.

4. Eigenvalues of the Transfer Matrix

In order to calculate thermodynamic functions the largest eigenvalue of the transfer matrix given in equation (9) is required. In the general case this must be obtained numerically. However, we have considered two particular relevant cases where it is unusually possible to extract all the eigenvalues of the transfer Matrix analytically by exploiting some properties of symmetrical matrices.

Consider the symmetrical matrix eigenvalue-eigenvector relationship

$$\begin{pmatrix} f_1 & \cdots & (f_1f_j)^{1/2} \\ \vdots & \ddots & \vdots \\ (f_jf_1)^{1/2} & \cdots & f_j \end{pmatrix}\begin{pmatrix} c_1 \\ \vdots \\ c_j \end{pmatrix}_k = \lambda_k \begin{pmatrix} c_1 \\ \vdots \\ c_j \end{pmatrix}_k \tag{14}$$

By inspection it may be observed that one of its eigenvalues and associated eigenvector satisfies

$$\begin{pmatrix} f_1 & \cdots & (f_1f_j)^{1/2} \\ \vdots & \ddots & \vdots \\ (f_jf_1)^{1/2} & \cdots & f_j \end{pmatrix}\begin{pmatrix} f_1^{1/2} \\ \vdots \\ f_j^{1/2} \end{pmatrix} = (\sum_{i=1}^{j} f_i)\begin{pmatrix} f_1^{1/2} \\ \vdots \\ f_j^{1/2} \end{pmatrix} \tag{15}$$

The standard rules for the inner product of 2 conformable square matrices can be used to show that since the maximum eigenvalue is $\lambda_{\max} = (\sum_{i=1}^{j} f_i)$ then all the other eigenvalues are zero. We have the relations

$$Tr\begin{pmatrix} f_1 & \cdots & (f_1 f_j)^{1/2} \\ \vdots & \ddots & \vdots \\ (f_j f_1)^{1/2} & \cdots & f_j \end{pmatrix}^2 = \sum_{m,n} f_m f_n = \sum_{k=1}^{j} (\lambda_k)^2 \qquad (16)$$

Since

$$\sum_{k=1}^{j} (\lambda_k)^2 = \sum_{m,n} f_m f_n = {\lambda_{\max}}^2 \qquad (17)$$

and since all the eigenvalues of a symmetrical matrix are real then all the other eigenvalues of the transfer matrix in equation(14) are zero.

5. Sharp Transitions (Model A) and Gradual Transitions (Model B) from phase mixtures in a sample

We consider mixed LP, NP and phase separated behaviour and discuss eigenvalues in both cases.

The matrix $\mathbf{A}$ (equation (9)) can be partitioned into two diagonal blocks which deal with LP and NP configurations and off-diagonal blocks which describe the coupling between these two types of configurations as shown below

$$\begin{pmatrix} \mathbf{A}_{LP,LP} & \mathbf{A}_{LP,NP} \\ \mathbf{A}_{NP,LP} & \mathbf{A}_{NP,NP} \end{pmatrix} \qquad (18)$$

The neglect or inclusion of the off-diagonal blocks leads to two models A and B.

If we follow Coudert and co-workers[54] and assume that LP and NP phases do not co-exist in a perfect sample then the off-diagonal couplings disappear giving the matrix

$$\begin{pmatrix} \mathbf{A}_{LP,LP} & 0 \\ 0 & \mathbf{A}_{NP,NP} \end{pmatrix} \qquad (19)$$

The LP and NP blocks in this equation decouple and this allows a study to be made of homogenous and inhomogenous systems. This we call model A.

Inclusion of this coupling allows for short range ordered phase mixtures in a sample which we name as model B.

We will discuss results for both models which may arise in various experimental situations depending on the sample history.

6. Adsorption Isotherms of Pure Methane and Pure Carbon Dioxide

Adsorption isotherms have been measured by Boutin et al[52] for CH_4 and CO_2 on MIL(53) Al. The energies of adsorption of the pure components and maximum occupations for the large and narrow pores are parameterized are shown in Table 1. Δ (chosen as 2.5 kJ/mol) is the energy difference between the LP and NP states and is the energy required to convert from the more stable LP to NP. They are effective energies valid in the approximate temperature range 200-300 K but we do not expect them to accurately reflect such parameters for a 3 dimensional MOF crystal.

It can be seen in Fig.2 that a satisfactory reproduction of the shape and temperature dependence is obtained when compared with the adsorption experimental isotherms of Boutin et al[52]. The isotherms from Model A are sharp and similar to first order phase transitions. Model A forbids the coexistence of large and narrow pores and corresponds to a thermodynamic NP/LP phase transition as postulated by Coudert and co-workers[54] where all narrow pores convert to large pores or vice versa at once. The isotherms predicted by Model B on the other hand are more rounded. Model B allows coexistence of both types of pores meaning that the NP/LP transition takes place at individual pore level rather than collectively.

Model A (sharp transition approach) predicts breathing, NP/LP transition, for pure carbon dioxide adsorption at the whole studied temperature range (204-320 K) as indicated by the sharp rises of adsorbed carbon dioxide amount. The transition pressure increases with temperature. For pure methane adsorption at 183 and 213 K, Fig. 2 (top – Model A) shows NP/LP transition at pressures below 2 bar. However, Model A predicts NP/LP transition at higher pressures, above the figure scale, for methane adsorption also at higher temperatures. At 273 K the original LP structure undergoes transition to NP at near zero bars, similarly to lower temperatures of 183 and 213 K, and at around 9 bar the NP structure undergoes transition back to LP. We have retained the pressure scale in the figure to 6 bar which is the same as the experimental literature isotherms[37] to enable direct comparison.

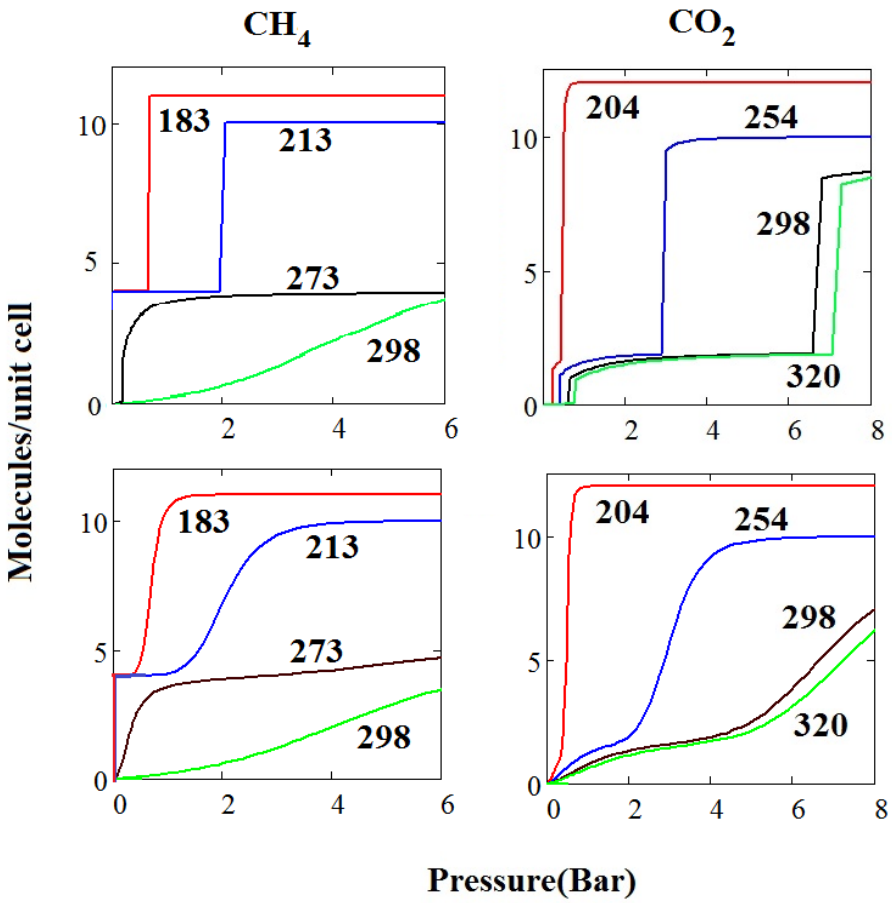

Figure 2 Adsorption isotherms of pure methane (on the left) and pure carbon dioxide (on the right) calculated using model A, sharp transition approach (two top diagrams) and model B, gradual transition approach (two lower diagrams). The curves are labelled with absolute temperature

Calculations of MOF volumes and adsorption isotherms was performed straightforwardly using the above methodology and the Mathcad 15 software package[55]. Finite difference calculation of derivatives was performed.

7. Adsorption Isotherms of Methane/ Carbon Dioxide Mixtures

Using the parameters for the pure single components, binary mixture isotherms of methane – carbon dioxide were calculated using both approaches, sharp transition, Model A and gradual transition, Model B at various carbon dioxide mole fractions (0, 0.2, 0.5, 0.8 and 1) are presented in Figs. 3 and 4 for 294 K and 304 K respectively. To reproduce the essential features of the mixture isotherms of Baron and co-workers[37] and also the equimolar mixture isotherm of Gomez et al[40], we have adjusted the interaction parameter J_{ab} to 198*k* indicating that CH_4 and CO_2 molecules in a pore experience an effective repulsion possibly due to competition for same binding sites.

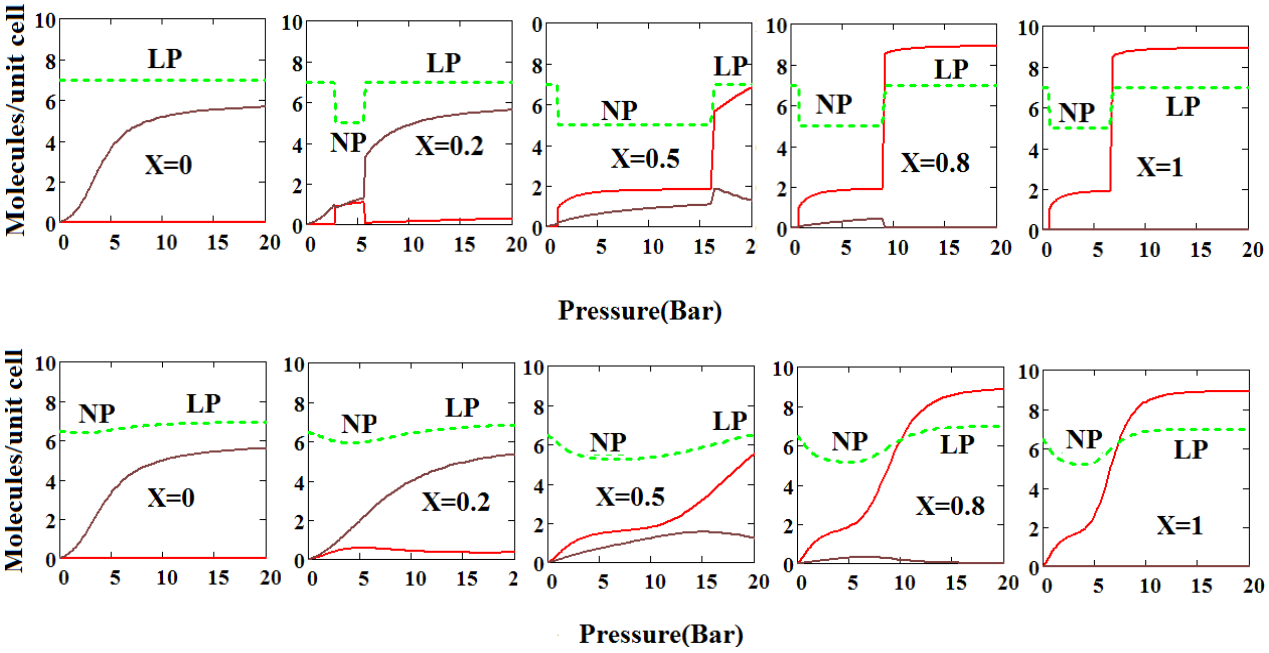

Fig 3 Methane-Carbon Dioxide mixture adsorption isotherms at various Carbon Dioxide mole fractions at 294 K. Top five isotherms are predicted using Model A, sharp transition approach, while bottom five isotherms are predicted using Model B, gradual transition approach. Methane- black curve ,Carbon Dioxide-red curve. The dotted green curve indicates the NP/LP state of the MOF.

For methane no LP to NP transition takes place (breathing) at 294K with the methane pressure below 20 bar. At 20 % gas carbon dioxide a LP to NP transition takes place in a narrow window from around 2.5 bar to just above 5 bar with carbon dioxide being adsorbed and immediately displaced by methane when the reverse NP to LP transition occurs. At 50%-50% gas mixtures the pressure range of NP existence is the largest (1-15 bar) with methane being dominantly adsorbed in the narrow pore. When the transition is reverses from the NP back to LP both component adsorbed amounts increase sharply with the adsorbed carbon dioxide rise sharper. As the pressure increases further carbon dioxide displaces methane from the large pore. Similar behavior, albeit gradual rather than sharp rises, is observed with Model B. The LP/NP transitions are gradual rather than sharp with the corresponding pressures where changes happen being similar to the very well defined pressure values of the sharp transitions of Model A. It is interesting to remark that the X=0.5 isotherm shown in Fig. 3, Model B is very close in form to that reported by Llewelyn and co-workers[28] for MIL53 (Cr). In particular, the carbon dioxide component shows a plateau up to about 10 bar as seen experimentally.

Comparing the mixture isotherms, at the slightly higher temperature of 304 K (Fig 4) we can see that NP to LP transitions occur at higher carbon dioxide gas mole fractions, corresponding to higher partial pressures. At 20 % carbon dioxide no LP to NP transition takes place.

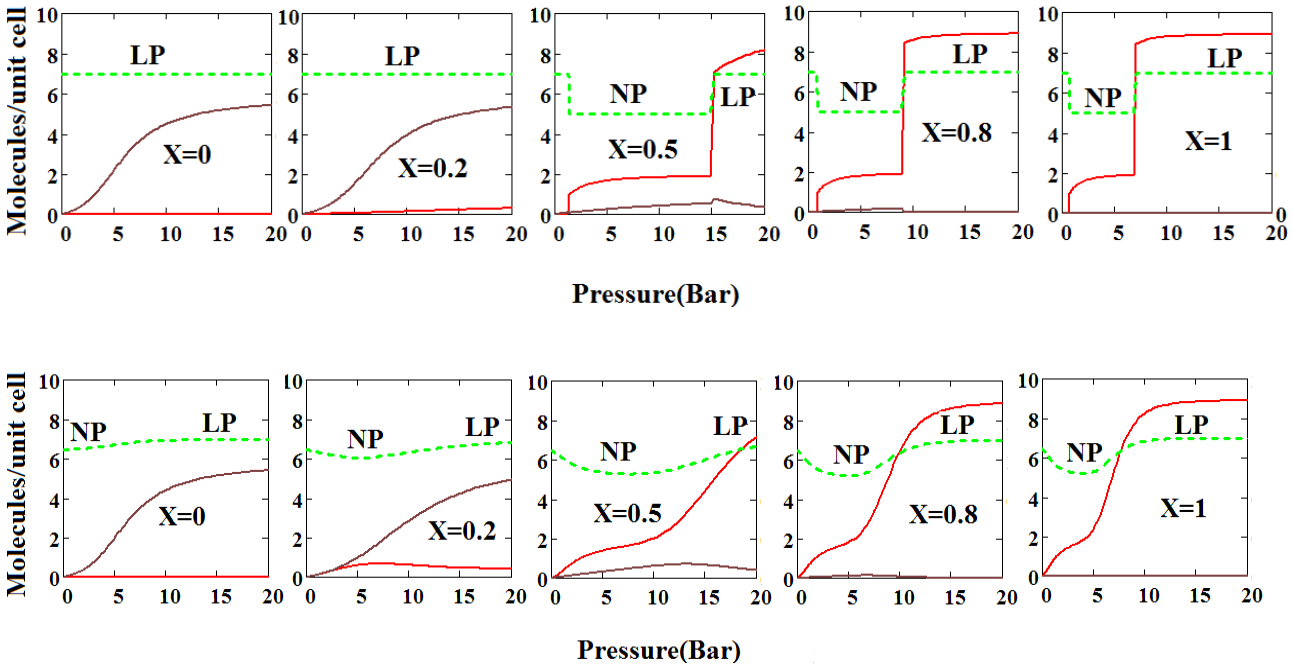

Fig 4 Methane-Carbon Dioxide mixture adsorption isotherms at various Carbon Dioxide mole fractions at 304 K. Top five isotherms are predicted using Model A, sharp transition approach, while bottom five isotherms are predicted using Model B, gradual transition approach. Methane- black curve ,Carbon Dioxide-red curve. The dotted green curve indicates the NP/LP state of the MOF.

8. Binary Mixture Adsorption as Function of Gas Phase Composition

In order to reproduce the Baron and co-workers[37] experimental mixture results, we have calculated adsorbed amounts against carbon dioxide gas mole fraction curves at 1 and 7.5 bar (Fig. 5, note the different Y axis/adsorption scales) using the parameters for the pure single components and using both Models A (Lower part) and B (Upper part).

The agreement of Model B (gradual transition approach) results with the experimental data is reasonably good. The apparent inconsistency of Model A predictions could be simply explained by the fact that the LP/NP transition occurs at all mole fractions at pressures above 7.5 bar, Fig. 4, upper part. At 1 bar (Fig. 5, lower part, left) the LP to NP transition occurs at a gas phase carbon dioxide mole-fraction of around 0.25. At 0-0.25 mole-fractions, the structure exists at LP of low occupation and at higher mole fractions 0.25–1 the structure exists at NP. The Model B 1 bar adsorption (Fig. 5, upper part, left) is the rounded adsorption curve version of Model A. At 7.5 bar (Fig. 5, lower part, right), the LP to NP transition occurs at a gas phase carbon dioxide mole-fraction of around 0.55. At 0-0.55 mole-fractions, the structure exists at LP of low occupation and at higher mole fractions 0.55–1 the structure exists at NP. At pressures above 7.5 bar, a reverse transition from NP to LP occurs (Fig. 4, upper part) leading to higher adsorption. Considering the

higher adsorbed amounts at higher pressures, Model B 7.5 bar adsorption (Fig. 5, upper part, right) is the rounded adsorption curve version of Model A.

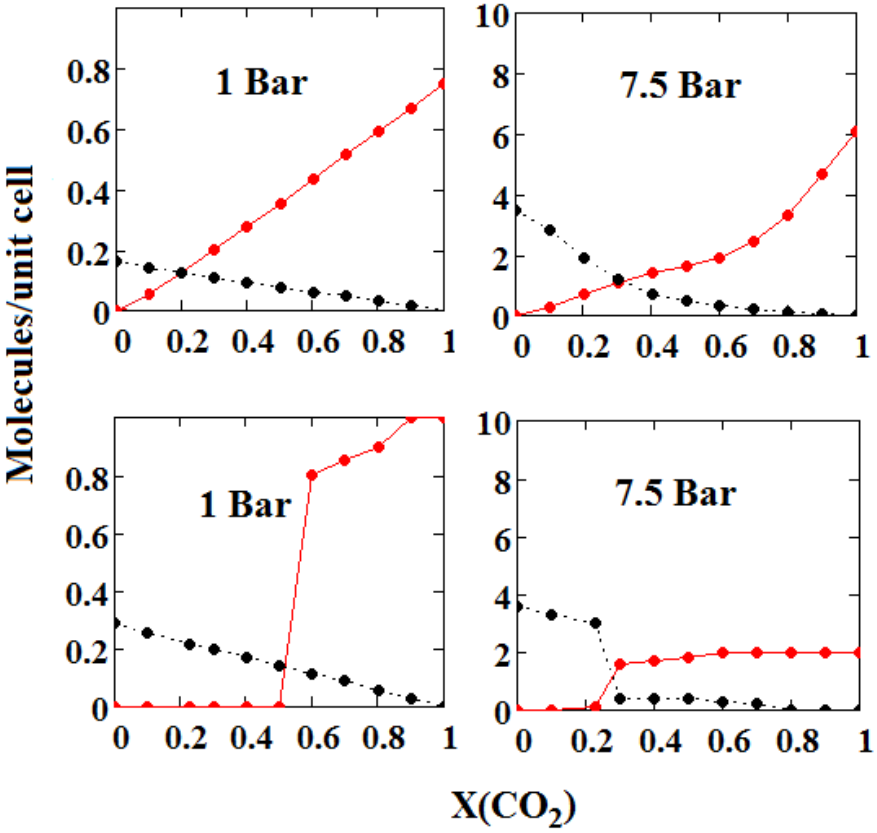

Fig 5 Binary mixture adsorption vs. gas phase carbon dioxide mole fraction calculated using Model A (lower) and Model B (upper) at 304 K and total pressures of 1 bar (left) and 7.5 bar (right). Methane- black, Carbon Dioxide-red.

9. Mixture Co-adsorption Phase Diagrams for Methane/Carbon Dioxide Mixtures.

We have used the results of our Model A (sharp transition approach) calculations to construct the mixture co-adsorption phase diagrams at three temperatures, 284, 294 and 304 K (Fig. 6) similarly to the experimental and theoretical study of Coudert and co-workers[39]. In Fig. 6 the pressure is plotted against gas phase carbon dioxide mole fraction at which NP/LP transitions take place, enabling to record areas of LP and NP existence. Blue areas indicate NP existence while yellow areas indicate LP existence. It should also be noted that the pressure scale at 284 K is different from the scale at 294 and 304 K. Furthermore, red horizontal lines indicate the pressure upper limit of NP existence while purple vertical lines indicate the carbon dioxide mole-fraction low limit of NP existence. The essential features of the calculated co-adsorption phase diagrams are in good agreement with Coudert and co-workers' results[39].

The carbon dioxide mole-fraction low limit decreases as temperature decreases. At 284 K, in this model the system breathes in pure methane, whereas experimentally MIL-53(Al) breaths in pure methane below 245 K[52].

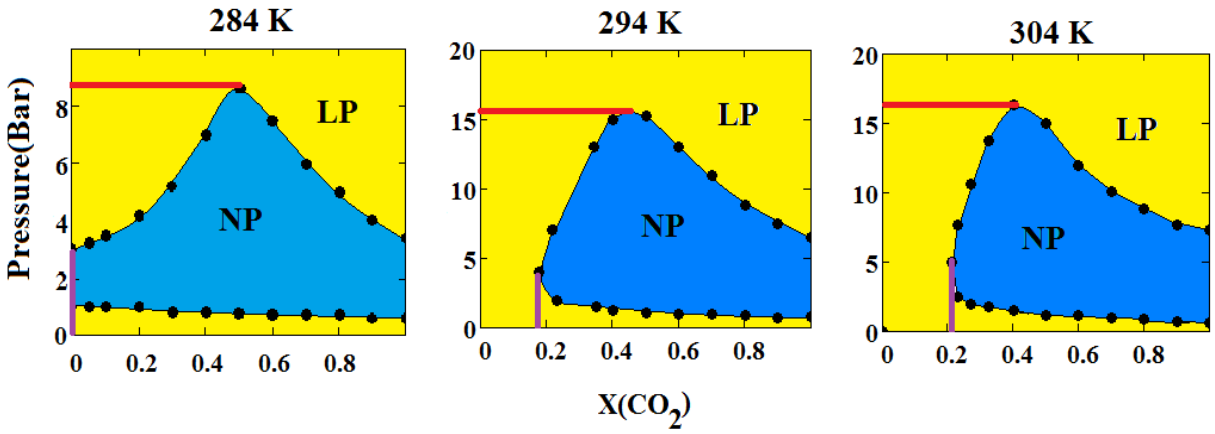

Fig 6 Mixture co-adsorption phase diagrams at 284, 294 and 304 K**. The red horizontal line and vertical purple line indicate the pressure and carbon dioxide mole fraction limits of NP existence.**

10. Role of Mechanical Pressure

Finally, we calculated using Model A (sharp transition approach) adsorption isotherms when the MOF structure is subjected at a constant mechanical pressure of 300 bar at various gas phase compositions, Fig. 7. Additionally to the gas phase pressure, the MOF structure is subjected to a purely mechanically applied pressure resulting in a total mechanical pressure of σ as illustrated in Fig. 1. The gas pressure is included in the total mechanical pressure. As the gas pressure changes, the applied mechanical pressure stays constant at σ = 300 bar.

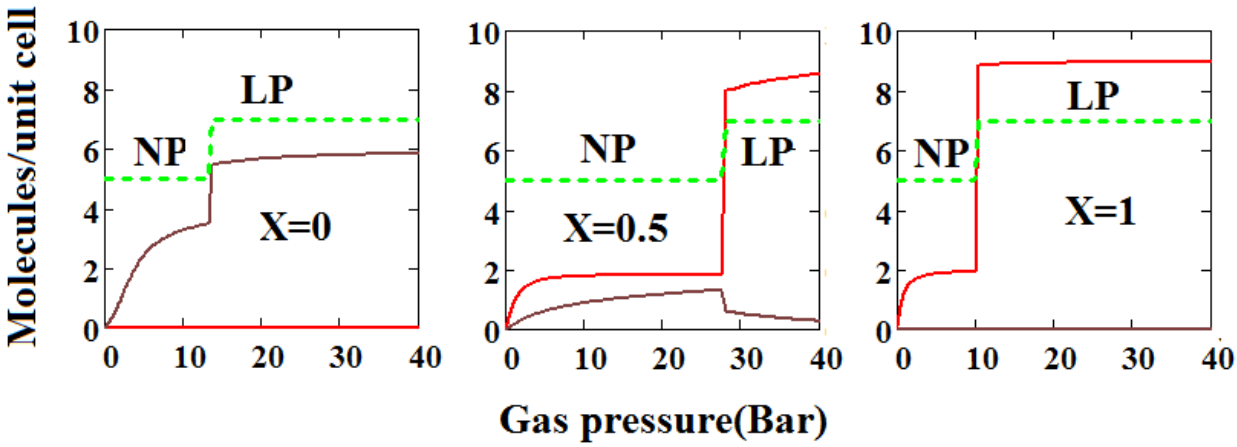

Fig. 7 Methane and carbon dioxide mixture adsorption isotherms at various carbon dioxide mole fractions (X) using model A, sharp transition approach under a mechanical pressure of

300 bar at 294 K. Methane- black curve ,Carbon Dioxide-red curve. The dotted green curve indicates the NP/LP state of the MOF.

The isotherms in Fig. 7 under mechanical pressure of 300 bar should be compared with those in Fig. 3, Upper Part, where no additional purely mechanical pressure is applied and therefore the total mechanical pressure is equal to the gas phase pressure.

Under a mechanical pressure of 300 bar, breathing occurs at 294 K at all gas phase compositions, even for pure methane. The additionally applied mechanical pressure compresses the MOF structure into the NP configuration at zero gas pressure. The gas adsorption triggers the NP to LP transition with corresponding sharp rises of adsorbed amounts. In the 50-50 % mixture the NP to LP transition leads to displacement of adsorbed methane by carbon dioxide, similarly to Fig. 3. Much interesting work seems possible regarding the influence of mechanical pressure on adsorption isotherms in MOFs

11. Conclusions

In this paper we have discussed the development of an exactly soluble lattice model of binary gas mixture adsorption in MOFs in the osmotic ensemble and present its application on methane - carbon dioxide system using the model parameters for the pure single components. The trends in the calculated pure component and mixture isotherms are in good agreement with experimental behaviour. In particular, the model is able to predict adsorption induced narrow/large pore transitions. Using the transfer matrix treatment and partioning of the matrix into two parts, LP/NP configurations and off-diagonal blocks, we have presented two models for binary mixture adsorption model, depending upon neglect (Model A) or inclusion (Model B) of the off-diagonal couplings. Model A forbids the coexistence of narrow and large pores leading to sharp transitions, while Model B allows the coexistence of both pore types leading to gradual transitions.

Furthermore, we have used the model to reproduce mixture co-adsorption phase diagrams for methane/ carbon dioxide at various temperatures which are found to give a good description of the experimental trends. Finally, we have investigated the effect of the mechanical pressure on the methane – carbon dioxide mixture adsorption isotherms. The mechanical pressure of 300 bar compresses the MOF structure into the narrow pore configuration, thus widening the range of conditions where narrow/large pore transition occur.

Overall, it seems that the model reproduces the trends in the experimentally observed behaviour of MOFs undergoing binary mixture adsorption. The predictions are not particularly sensitive to the choice of model parameters. Much work remains possible regarding the influence of mechanical

pressure on adsorption isotherms in MOFs. Further work is underway to develop a three-dimensional model of binary mixture adsorption in MOFs treated by mean-field theory.

Competing Interests

The authors have no competing interests.

Authors' Contributions

Both authors contributed equally to the design this study and drafting of the manuscript. They also participated equally to the theoretical developments and analysis and calculation of results. Both gave final approval for publication.

References

[1] Dunne LJ, Murrell JN, Manos G. Exact statistical mechanical lattice model and classical Lindemann theory of melting of inert gas solids. *Chemical Physics Letters* **456**, 162-165 (doi: 10.1016/j.cplett.2008.03.025)

[2] Dunne LJ, Murrell JN, Manos G, Rekabi M, 2006, Exact matrix computation of the statistical mechanics of a cell model of hard sphere phase behavior. *Chemical Physics Letters* **421**, 47-51 (doi: 10.1016/j.cplett.2006.01.032)

[3] Dunne LJ, Murrell JN, Brändas EJ. Off-diagonal long range order from repulsive electronic correlations in the ground state of a two-dimensional localised model of a high-Tc cuprate superconductor *Physica C: Superconductivity and Its Applications* **169**, 501-507 (doi: 10.1016/0921-4534(90)90598-9)

[4] Suzuki S, Messaoud SB, Takagaki A, Sugawara T, Kikuchi R, Oyama ST, 2014, Development of inorganic–organic hybrid membranes for carbon dioxide/methane separation. *Journal of Membrane Science*, **471**, 402-411 (doi: 10.1016/j.memsci.2014.08.029)

[5] Yeo ZY, Chai S-P, Zhu PW, Mohamed AR, 2014, Development of a hybrid membrane through coupling of high selectivity zeolite T on ZIF-8 intermediate layer and its performance in carbon dioxide and methane gas separation. *Microporous and Mesoporous Materials*, **196**, 79-88 (doi: 10.1016/j.micromeso.2014.05.002)

[6] Jensen NK, Rufford TE, Watson G, Zhang DK,Chan KI, May EF, 2012, Screening Zeolites for Gas Separation Applications Involving Methane, Nitrogen, and Carbon Dioxide. *J. Chem. Eng. Data*, **57**, 106–113 (doi: 10.1021/je200817w)

[7] Venna SR, Carreon MA, 2010, Highly Permeable Zeolite Imidazolate Framework-8 Membranes for CO_2/CH_4 Separation. *J. Am. Chem. Soc.*, 132, 76–78 (doi: 10.1021/ja909263x)

[8] Lu LH, Wang SS, Muller EA, Cao W, Zhu YD, Lu XH, Jackson G, 2014 Adsorption and separation of CO_2/CH_4 mixtures using nanoporous adsorbents by molecular simulation. *Fluid Phase Equilibria*, **362**, 227-234 (doi: 10.1016/j.fluid.2013.10.013)

[9] Huck JM, Lin LC, Berger AH, Shahrak MN, Martin RL, Bhow AS, Haranczyk M, Reuter K, Smit B, 2014, Evaluating different classes of porous materials for carbon capture. *Energy & Environmental Science*, **7**, 4132-4146 (doi: 10.1039/c4ee02636e)

[10] Manos G, Dunne LJ, Jalili S, Furgani A, Neville T, 2012, Monte Carlo Simulation and Exact Statistical Mechanical Lattice Models as a Development Tool for Zeolite Multi-Component Adsorption Isotherm Derivation. *Adsorption Science and Technology* **30**, 503-519 (doi: 10.1260/0263-6174.30.6.503)

[11] Horike S, Shimomura S, Kitagawa S, 2009, Soft Porous Crystals. *Nat. Chem.* **1**, 695-704

[12] Bozbiyik B, Duerinck T, Lannoeye J, De Vos DE, Baron GV, Denayer JFM, 2014, Adsorption and separation of n-hexane and cyclohexane on the UiO-66 metal-organic framework. *Microp. Mesop. Mater.* **183**, 143-149. (doi: 10.1016/j.micromeso.2013.07.035)

[13] Duerinck T, Bueno-Perez R, Vermoortele F, De Vos DE, Calero S, Baron GV, Denayer JFM, 2013, Understanding Hydrocarbon Adsorption in the UiO-66 Metal-Organic Framework: Separation of (Un)saturated Linear, Branched, Cyclic Adsorbates, Including Stereoisomers. *J. Phys. Chem. C* **117**, 12567-12578. (doi: 10.1021/jp402294h)

[14] Zhao Z, Ma X, Kasik A, Li Z, Lin YS, 2013, Gas Separation Properties of Metal Organic Framework (MOF-5) Membranes. *Ind. Eng. Chem. Res.***52**, 1102-1108.

[15] Li J-R, Kuppler RJ, Zhou H-C, 2009, Selective gas adsorption and separation in metal–organic frameworks. *Chem. Soc. Rev.*, **38**, 1477-1504. (doi: 10.1039/B802426J)

[16] Car A. Stropnik C. Peinemann K-V. 2006, Hybrid membrane materials with different metal–organic frameworks (MOFs) for gas separation. *Desalination*, **200**, 424-426. (doi: 10.1016/j.desal.2006.03.390)

[17] Zornoza B, Martinez-Joaristi A, Serra-Crespo P, Tellez C, Coronas J,Gascon J, Kapteijn F, 2011, C*hem. Commun.***, 47**, 9522-9524. (doi: 10.1039/C1CC13431K)

[18] Li B, Wang H, Chen B, 2014, Microporous Metal–Organic Frameworks for Gas Separation. *Chemistry An Asian Journal*, **9**, 1474–1498. (doi: 10.1002/asia.201400031)

[19] Pimentel BR, Parulkar A, Zhou E-k, Brunelli NA, Lively RP, 2014, Zeolitic Imidazolate Frameworks: Next-Generation Materials for Energy-Efficient Gas Separations. *ChemSusChem* 7, 3202–3240. (doi: 10.1002/cssc.201402647)

[20] Bendt S, Hovestadt M, Böhme U, Paula C, Döpken M, Hartmann M, Keil FJ, 2016, Olefin/Paraffin Separation Potential of ZIF-9 and ZIF-71: A Combined Experimental and Theoretical Study. *Eur J Inorg Chem*, **2016**, 4440–4449. (doi: 10.1002/ejic.201600695)

[21] Lin Y, Kong C, Zhang Q, Chen L, 2017, Metal-Organic Frameworks for Carbon Dioxide Capture and Methane Storage. *Advanced Energy Materials*, **7**, 1601296 (doi: 10.1002/aenm.201601296)

[22] Couck S, Van Assche TRC, Liu Y_Y, Baron GV, Van Der Voort P, Denayer JFM, 2015, Adsorption and Separation of Small Hydrocarbons on the Flexible, Vanadium-Containing MOF, COMOC-2. *Langmuir*, **31**, 5063–5070. (doi: 10.1021/acs.langmuir.5b00655)

[23] Hess SC, Grass RN, Stark WJ, 2016, MOF Channels within Porous Polymer Film: Flexible, Self-Supporting ZIF-8 Poly(ether sulfone) Composite Membrane. *Chem. Mater.*, **28**, 7638–7644. (doi: 10.1021/acs.chemmater.6b02499)

[24] Sarkisov L, Martin RL, Haranczyk, M.; Smit, B. On the Flexibility of Metal− Organic Frameworks. *J. Am. Chem. Soc.*, **2014**, *136*, 2228−2231. (doi: 10.1021/ja411673b)

[25] Kanoo P, Gurunathaa KL, and Maji TK, 2010, Versatile functionalities in MOFs assembled from the same building units: interplay of structural flexibility, rigidity and regularity. *J. Mater. Chem.*, **20**, 1322-1331. (doi: 10.1039/B917029D)

[26] Salles F, Ghoufi A, Maurin G, Bell RG, Mellot-Draznieks C, Férey G, 2008, Molecular Dynamics Simulations of Breathing MOFs: Structural Transformations of MIL-53(Cr) upon Thermal Activation and CO2 Adsorption. *Angewandte Chemie*, **120**, 8615–8619. (doi: 10.1002/ange.200803067)

[27] Lin Z-J, Lü J, Hong M, Cao R, 2014, Metal–organic frameworks based on flexible ligands (FL-MOFs): structures and applications. *Chem. Soc. Rev.*, **43**, 5867-5895. (doi: 10.1039/C3CS60483G)

[28] Thomas Devic T, Salles F, Bourrelly S, Moulin B, Maurin G, Horcajada P, Serre C, Vimont A, Lavalley J-C, Leclerc H, Clet G, Daturi M, Llewellyn PL, Filinchuk Y, Fereya G, 2012, Effect of the organic functionalization of flexible MOFs on the adsorption of CO2. *J. Mater. Chem.*, **22**, 10266-10273. (doi: 10.1039/c2jm15887f)

[29] Chen L, Mowat JPS, Fairen-Jimenez D, Morrison CA, Thompson, SP, Wright PA, Düren T, 2013, Elucidating the Breathing of the Metal−Organic Framework MIL-53(Sc) with ab Initio Molecular Dynamics Simulations and in Situ X‑ray Powder Diffraction Experiments. *J. Am. Chem. Soc.* **135**, 15763−15773. (doi:10.1021/ja403453g)

[30] Llewellyn PL, Maurin G, Devic T, Loera-Serna S, Rosenbach N, Serre C, Bourrelly S, Horcajada P, Filinchuk Y, Ferey G, 2008 Prediction of the Conditions for Breathing of Metal Organic Framework Materials Using a Combination of X-ray Powder Diffraction, Microcalorimetry, and Molecular Simulation. *J. Am. Chem. Soc.* **130**, 12808–12814. (doi:10.1021/ja803899q)

[31] Coudert F_X, Boutin A, Fuchs AH, Neimark AV, 2013, Adsorption Deformation and Structural Transitions in Metal–Organic Frameworks: From the Unit Cell to the Crystal. J. Phys. Chem. Lett., **4**, 3198–3205. (doi: 10.1021/jz4013849)

[32] Neimark, A. V.; Coudert F-X, Triguero C, Boutin A, Fuchs AH, Beurroies I, Denoyel R, 2011, Structural Transitions in MIL-53 (Cr): View from Outside and Inside. *Langmuir* **27**, 4734-4741. (doi: 10.1021/la200094x)

[33] Neimark AV, Coudert F-X, Boutin A, Fuchs AH, 2010, Stress-Based Model for the Breathing of Metal−Organic Frameworks. *J. Phys. Chem. Lett.*, **1**, 445–449. (doi: 10.1021/jz9003087)

[34] Ortiz AU, Boutin A, Fuchs AH, Coudert F-X, 2012, Anisotropic Elastic Properties of Flexible Metal–Organic Frameworks: How Soft are Soft Porous Crystals? *Phys. Rev. Lett.*, **109**, 195502

[35] D. Fairen-Jimenez D, Moggach SA, Wharmby MT, Wright PA, Parsons S, T. Duren T, 2011, Opening the Gate: Framework Flexibility in ZIF-8 Explored by Experiments and Simulations. *J. Am. Chem. Soc.* **133**, 8900–8902. (doi: 10.1021/ja202154)

[36] Bousquet D, Coudert F-X, Fossati AGJ, Neimark AV, Fuchs AH, Boutin A, 2013, Adsorption induced transitions in soft porous crystals: An osmotic potential approach to multistability and intermediate structures. *J Chem Phys* **138**, 174706 (doi: http://dx.doi.org/10.1063/1.4802888)

[37] Finsy V, Ma L, Alaerts L, De Vos DE, Baron GV, Denayer JFM, 2009, Separation of CO2/CH4 mixtures with the MIL-53(Al) metal–organic framework. *Microporous and Mesoporous Materials*, **120**, 221-227 (doi: :10.1016/j.micromeso.2008.11.007)

[38] Coudert F-X, 2010, The osmotic framework adsorbed solution theory: predicting mixture co-adsorption in flexible nanoporous materials. *Phys. Chem. Chem. Phys.*, **12**, 10904-10913. (doi: 10.1039/C003434G)

[39] Ortiz AU, Marie-Anne Springuel-Huet M-A, Coudert F-X, Fuchs AH, Boutin A, 2012, Predicting Mixture Co-adsorption in Soft Porous Crystals: Experimental and Theoretical Study of CO2/CH4 in MIL-53(Al) *Langmuir*, **28**, 494–498 (doi: 10.1021/la203925y)

[40] Gomez LF, Zacharia R, Bénard P, Chahine R, 2015, Simulation of Binary CO_2/CH_4 Mixture Breakthrough Profiles in MIL-53 (Al), *Journal of Nanomaterials*, **2015,** 439382 (doi: 10.1155/2015/439382)

[41] Bae Y-S, Mulfort KL, Frost H, Ryan P, Punnathanam S, Broadbelt LJ, Hupp JT, Snurr RQ, 2008, Separation of CO_2 from CH_4 Using Mixed-Ligand Metal−Organic Frameworks. *Langmuir*, 2008, **24**, 8592–8598 (doi: 10.1021/la800555x)

[42] Brennan JK, Madden WG, 2002, Phase Co-existence Curves for Off-Lattice Polymer−Solvent Mixtures: Gibbs-Ensemble Simulations *Macromolecules*, **35**, 2827-2834. (doi:10.1021/ma0112321)

[43] Panagiotopoulos AZ, 1987, Direct determination of phase co-existence properties of fluids by Monte Carlo simulation in a new ensemble. *Molecular Physics*, **61**, 813- 826 (doi:10.1080/00268978700101491)

[44] Dunne LJ, Manos G, 2015, Exact Matrix Treatment of Statistical Mechanical Lattice Model of Adsorption Induced Gate Opening in Metal Organic Frameworks. *Journal of Statistical Mechanics: Theory and Experiment*, P05008 (doi: 10.1088/1742-5468/2015/05/P05008)

[45] Dunne LJ, Manos G, 2016, Exact Matrix Treatment of an Osmotic Ensemble Model of Adsorption and Pressure Induced Structural Transitions in Metal Organic Frameworks. *Dalton Transactions*, **45**, 4213–4217 (doi: 10.1039/c5dt03248b)

[46] Coudert F-X, Jeffroy M, Fuchs AH, Boutin A, Mellot-Draznieks C, 2008, Thermodynamics of Guest-Induced Structural Transitions in Hybrid Organic−Inorganic Frameworks. *J. Am. Chem. Soc.* **130**, 14294-14302. (doi: 10.1021/ja805129c)

[47] Coudert F-X, Mellot-Draznieks C, Fuchs AH, and Boutin A, 2009, Double Structural Transition in Hybrid Material MIL-53 upon Hydrocarbon Adsorption: The Thermodynamics Behind the Scenes. *J. Am.Chem. Soc.*, **131**, 3442-3443. (doi: 10.1021/ja8094153)

[48] Hill TL, *Statistical Mechanics*. McGraw Hill, New York, 1956

[49] T. L. Hill, *An Introduction to Statistical Thermodynamics*; Addison-Wesley: New York, U. S. A., 1960. P.80

[50] Manos G, Du L, Dunne LJ (2010) "Statistical Mechanical Lattice Model Studies of Adsorption in Nanochannels Treated by Exact Matrix Methods" Chapter 6 in "Adsorption and Phase Behaviour in Nanochannels and Nanotubes" (Eds: L.J. Dunne, G. Manos), Springer Publishers, 121-145

[51] Simon CM, Braun E, Carraro C, Smit B, 2017, Statistical mechanical model of gas adsorption in porous crystals with dynamic moieties. *Proceedings of the National Academy of Sciences of the United States of America*, **114**, E287-E296 (doi: 10.1073/pnas.1613874114)

[52] Boutin A, Coudert F-X, Springuel-Huet M-A, Neimark AV, Férey G, Fuchs AH**,** 2010**,** The Behavior of Flexible MIL-53(Al) upon CH4 and CO2 Adsorption. *J. Phys. Chem. C*, **114**, 22237–22244 (doi: 10.1021/jp108710h)

[53] M.Rigby, E.B Smith, W.A.Wakeham and G.C Maitland , *The Forces Between Molecules*, Oxford University Press,1986

[54] Bousquet D, Coudert F-X, Boutin A, 2012, Free energy landscapes for the thermodynamic understanding of adsorption-induced deformations and structural transitions in porous materials. *J. Chem. Phys.*, **137**, 044118 (doi: 10.1063/1.4738776)

[55] The mathematical software used (Mathcad 15) is available from: Mathcad 15, Parametric Technology Corporation, 140 Kendrick Street, Needham, MA 02494 USA.